Egyptian Journal of Chemistry

http://ejchem.journals.ekb.eg/

Design, Molecular Docking, Synthesis and Evaluation of New Isatin Derivatives Bearing Pyridine Moiety as Potential Tyrosine Kinase Inhibitors

Noor Waleed Ibrahim, Monther Faisal Mahdi, Ayad M. R. Raauf

Department of Pharmaceutical Chemistry, College of Pharmacy, Mustansiriyah University, Baghdad-Iraq.

Abstract

A series of new 1-(3-imino-2-oxoindolin-5-yl)-3-phenylurea derivatives were synthesized starting from 5-aminoisatin; as a part of our program to compose multicomponent hybrid templates with potential pharmaceutical recognition and evaluate them as inhibitors of receptor tyrosine kinase. The proposed chemicals were synthesized and purified satisfactorily; They were classified and identified using a variety of methods: melting point, IR spectroscopy, ^{1}H-NMR and^{13}C-NMR; The effectiveness of these novel chemicals was tested for their *in vitro* cytotoxic activity and *In silico* tyrosine kinase selectivity through molecular docking via GOLD Suite (*v.5.7.1*); There is a good agreement between our docked results and the experimental results (*In vitro* study) since the compound 3a was the most potent cytotoxic scaffold shows the highest docking results and at the same time showing a promising antitumor activity among the tested compounds when tested against (A549) cancer cell lines by the MTT assay with IC_{50}= 30.4 µM in comparison with erlotinib. Furthermore, using SWISS ADME, the drug likeness of these selected anti-proliferative drugs was anticipated based on their pharmacokinetics profiles. By not violating Lipinski's rule of five, the anti-proliferative drugs were determined to be orally safe. This study proposed a method for developing effective anti-proliferative drugs that target their target enzyme.

Keywords: 5-Aminoisatin; Docking; ADME; GOLD; Lipinski rule.

1. Introduction

Due of their extensive biological profile, heterocyclic compounds are an important family of organic molecules, researchers are constantly exploiting these heterocyclic moieties, either alone or in their fused form, for the development of novel medications. Isatin(1H-indole-2,3-dione), also known as indole quinine and indenedione, is a nitrogen-containing heterocyclic molecule [1]. As a versatile molecule, isatin is the precursor of a huge number of derivatives, containing the oxindole moiety and presenting a wide range of biological and pharmacological properties such as antimicrobial activities , anticonvulsant activity, antiproliferative activity, anti-inflammatory activity, antioxidant activity, anthelmintic activity[2-7].

Tumours are abnormal tissue masses that are either solid or fluid-filled. Benign tumors are defined as tumors that grow only at the place of origin and have a normal physical appearance [8]. Cancerous cells, or malignant tumours, are defined as cells that are aberrant and can proliferate uncontrollably. Tumours are also referred to as neoplasms [9].

The accumulation of genetic and epigenetic changes leads to the development of human cancers[10].

Both mutations are now known to exist in cancer cells as well as normal ones long before cancer begins. Exposure to environmental factors is linked to specific patterns of changes.

A "field for cancerization (cancerization field)" is tissue that has accumulated abnormalities [11]. Cancer can take a long time to develop from start to finish. Because of the protracted development period, there may be a possibility to deploy multi-functional, multi-targeted preventative medications to stop or reverse carcinogenesis. Targeting and reversing early epigenetic changes could be one way to avoid cancer. They are possibly reversible, unlike genetic changes, and can be returned to their original state [12]. An

*Corresponding author e-mail: noorwaleed@uomustansiriyah.edu.iq; (Noor Waleed Ibrahim).
Receive Date: 17 April 2021, Revise Date: 19 August 2021, Accept Date: 01 September 2021
DOI: 10.21608/EJCHEM.2021.72747.3607

increase in natural and unnatural cancer-causing agents has played a relatively large part in increasing death rates across the world annually[13]. Although infectious diseases and cancers have different underlying aetiologies, from a pharmacologic perspective, the broad principles of treatment are similar. The targeting of selective differences between the microorganism or cancer cell and the normal host cell is a common thread in various pharmaceutical techniques. Because both microorganisms and cancer cells can develop resistance to medication treatments, finding new remedies is a never-ending effort [14]; Drug resistance is still a key roadblock to effective cancer treatment. Poor drug absorption and delivery, genetically driven variability in drug transport, activation, clearance, mutations, and amplifications or deletions in therapeutic targets are only some of the pharmacokinetic and molecular alterations that can render even the best-designed treatments ineffective and cause resistance [15]. The development of new and different cancer therapies provided the means for treating resistant cancer cells that previously had been susceptible to an older therapy [16], Our goal is to design and synthesize the best-fit structures as new tyrosine kinase inhibitors using soft wares and anticancer activity prediction using modern software provided by the Cambridge Crystallographic Data Centre, and to test those tyrosine kinase inhibitors on a specific cancer cell line culture (A549).

2. Material and methods

All reagents and anhydrous solvents were of analytical grade and generally used as received from the commercial suppliers (U.K., Spain, Germany, China, BDH and England). 5-Aminoisatin was supplied by the ChemShuttle Company, United States. Melting points were determined by open capillary method on Stuart/ Electrothermal an electric melting point apparatus (U.K.) and IR spectra were recorded on a FT-IR spectrophotometer Shimadzu as KBr disks at College of Pharmacy, Mustansiriyah University. ^{1}H NMR spectra were recorded using DMSO-d6 as solvent and TMS as internal standard on a Bruker(400 MHz)& Varian 500 MHz spectrometer (Chemical shifts represented in δ, ppm). ^{13}C NMR spectra were recorded on a Bruker (75.65 MHz))& Varian(125.65 MHz)) spectrometer. CCDC GOLD Suite (*v*.5.7.1) was utilized to perform the molecular docking researchs for the compounds. CCDC Hermes visualizer software (*v*. 1.10.1) was utilized to imagine: the protein, ligands, hydrogen bonding interactions, short contacts and bonds length calculation. The chemical structures of our ligands were drawn utilizing ChemBioOffice (*v*. 17.1) software. The pharmacokinetic profile, i.e., ADME of the synthesized compounds was anticipated with the assistance of swiss ADME server [17].

Cytotoxicity assay was performed at the tissue culture center/ pharmacology and toxicology department/ College of Pharmacy, Mustansiriyah University using trypsin/EDTA, RPMI 1640,fetal bovine serum (Fisher scientific , USA);

[MTT 3-(4,5-dimethyl-2-thiazolyl)-2,5-diphenyl -2H-tetrazoliumbromide] (Fisher scientific , USA); dimethyl sulfoxide (DMSO-SantacruzBiotechnology, Dallas, TX, USA);phosphate-buffered saline (PBS)(Gibco, USA);

CO_2 incubator and laminar flow hood (Memert, Germany); Autoclave (Astell, Germany); Freezer -20 ºC (Crafft, Korea); Freezer -80 ºC (Gel, Germany).

2.1. Chemical Synthesis (Scheme 1)

2.1.1. General procedure for the synthesis of 5-aminoisatin schiff bases (2a-d)

Pyridine amines (3 mmol) and 5-amino isatin hydrochloride (0.5958 gm, 3 mmol) were added to ethanol (10 mL) in a round bottomed flask, the mixture was heated during the first few minutes to a bout 50°C, then add 1 mL of glacial acetic acid drop by drop. The mixture was continued to be heated with stirring at 79 °C under reflux for 4 hrs; mixture cooled to room temperature. The resulting solid was collected by filtration, washed with absolute ethanol and dried in open air. The result compounds were added to solution of 3ml of (1.5 mmol, 0.0074 gm) K_2CO_3 dissolved in distilled water and after stirring for a few minutes was filtered; washed with water, dried and recrystallized from absolute ethanol[18].

6-((5-amino-2-oxoindolin-3-ylidene)amino)nicotinic acid (2a)

Physical properties: Red (75% yield); m.p. 184-185°C. FT-IR(KBr, cm^{-1}): 3358, 3271cm^{-1} ν (NH2 of isatin), 3188 cm^{-1} ν (NH), 3017 cm^{-1} ν (C-H aromatic), 1732 cm-1 ν (C=O), 1661 cm^{-1} ν (C=N), 1612 cm^{-1} ν (C=C aromatic) and 1313cm^{-1} ν(C-N).

^{1}H-NMR: 5.80ppm (s,2H, NH2), 6.48ppm (d,1H, Ar-H), 6.51ppm (d,1H, Ar-H), 6.92ppm (s,1H, Ar-H), 6.96ppm (d,1H, Ar-H), 7.86-7.82ppm (d,1H, Ar-

H), 8.52ppm (s,1H, Ar-H), 10.63 ppm (s,1H, NH) and 10.96ppm (s,1H,OH).

^{13}C-NMR:(107.82, 113.24, 113.77, 116.46, 123.72,127.44, 138.22, 144.62, 145.37, 151.12, 156.49, 162.73 and 163.67) ppm.

2-((5-amino-2-oxoindolin-3-ylidene)amino)nicotinamide (2b)

Physical properties: Reddish brown (71.4% yield); m.p. 180-183°C. FT-IR(KBr, cm^{-1}): 3410, 3285 cm^{-1} ν (NH2 of isatin), 3184 cm^{-1} ν (NH), 3003 cm^{-1} ν (C-H aromatic), 1734 cm^{-1} ν (C=O), 1661 cm^{-1} ν (C=N+C=O of amide), 1612 cm^{-1} ν (C=C aromatic) and 1311cm-1 ν(C-N).

^{1}H-NMR: 5.80ppm (s,2H, NH2), 6.61 ppm (d,1H, Ar-H), 6.92ppm (s,1H, Ar-H), 6.96ppm (t,1H, Ar-H), 6.98ppm (d,1H, Ar-H), 7.26ppm (s,2H, NH2 of amide), 7.96-7.99ppm (d,1H, Ar-H), 8.07-8.09ppm (d,1H, Ar-H) and 10.94ppm (s,1H,NH).

^{13}C-NMR:(111.73, 113.20, 113.81, 116.48, 123.65, 137.97, 144.59, 145.40, 151.02, 156.48 and 163.67) ppm.

5-amino-3-((5-(trifluoromethyl)pyridin-2-yl)imino)indolin-2-one (2c)

Physical properties: Red (77% yield); m.p. 192-194°C. FT-IR(KBr, cm^{-1}): 3445, 3204cm^{-1} ν (NH2 of isatin), 3225 cm^{-1} ν (NH), 1734 cm^{-1} ν (C=O), 1657 cm^{-1} ν (C=N), 1610 cm^{-1} ν (C=C aromatic), 1310cm^{-1} ν(C-N) and 843 cm-1 ν(C-F).

^{1}H-NMR: 5.80ppm (s,2H, NH2), 6.68 ppm (d,2H, Ar-H), 6.95ppm (s,1H, Ar-H), 6.96ppm (d,1H, Ar-H), 6.99ppm (d,1H, Ar-H), 10.62ppm (s,1H, Ar-H) and 10.95ppm (s,1H,NH).

^{13}C-NMR:(113.23, 113.79, 116.44,116.47, 123.68, 144.61, 145.35, 145.38,151.51, 156.48 and 163.67) ppm.

(Z)-5-amino-3-((4-(hydroxymethyl)pyridin-2-yl)imino)indolin-2-one(2d)

Physical properties: Reddish brown (69.5% yield); m.p. 170-173°C. FT-IR(KBr, cm^{-1}): 3458cm^{-1} ν (OH), 3391, 3310cm^{-1} ν (NH2 of isatin), 3208 cm^{-1} ν (NH), 3034 cm^{-1} ν (C-H aromatic),2924,2853 cm^{-1} ν (C-H aliphatic), 1734 cm^{-1} ν (C=O), 1659 cm^{-1} ν (C=N), 1612 cm^{-1} ν (C=C aromatic), 1310cm^{-1} ν(C-N).

^{1}H-NMR: 4.43ppm (s,1H, OH), 5.80ppm (s,2H, NH2), 6.67 ppm (s,2H, aliphatic CH2), 6.73ppm (d,1H, Ar-H), 6.92ppm (s,1H, Ar-H), 6.96ppm (s,1H, Ar-H), 6.99ppm (d,1H, Ar-H), 7.82ppm (d,1H, Ar-H)), 10.61ppm (d,1H, Ar-H) and 10.95ppm (s,1H,NH).

^{13}C-NMR:(62.11, 113.23, 113.78, 116.47, 123.70, 144.62, 145.38, 147.97, 156.49 and 163.67) ppm.

2.1.2. General procedure for the synthesis of ureido derivatives of 5- aminoisatin Schiff bases(3a-d&4a-d)

Compounds (2a-d) (1 mmol) was added to 10mL dichloromethane / methanol in a ratio of (9:1). The mixture was cooled to 10 ºC the appropriate substituted aromatic isocyanates (1mmol) was added slowly. The mixture was stirred at the room temperature for 4 hrs. and left in the refrigerator overnight. Solid product 3a-d&4a-d were separated out from the mixture, washed with dichloromethane, allowed to air dried and recrystallized from absolute ethanol[19].

6-((2-oxo-5-(3-(m-tolyl)ureido)indolin-3-ylidene)amino)nicotinic acid (3a)

Physical properties: Reddish orange (69% yield); m.p. 282°C dec. FT-IR(KBr, cm^{-1}): 3298, 3273 cm^{-1} ν (NH of urea&2-oxoindolin), 3042 cm^{-1} ν (C-H aromatic),2949, 2918 cm^{-1} ν(C-H aliphatic), 1734 cm^{-1} ν (C=O), 1634 cm^{-1} ν (C=N+C=O of urea), 1610 cm^{-1} ν (C=C aromatic), 1554 cm^{-1} ν (NH deformation in urea),1554 cm^{-1} ν (N-C-N) and 1294cm^{-1} ν(C-N).

^{1}H-NMR: 2.28ppm (s,3H, CH3), 6.78 ppm (d,2H, Ar-H), 6.80ppm (t,1H, Ar-H), 6.97ppm (s,1H, Ar-H), 7.15ppm (d,1H, Ar-H), 7.17ppm (d,2H, Ar-H)), 7.21ppm (s,1H, Ar-H) , 7.23ppm (d,1H, Ar-H) , 7.31ppm (s,1H, Ar-H) , 7.96ppm (s,1H, NH ureido) , 8.95 ppm (s,1H, NH ureido), 10.71ppm (s,1H,NH) and10.99ppm (s,1H,OH).

^{13}C-NMR:(21.86,106.56, 113.24, 113.77, 113.69, 116.46, 123.72, 127.44, 131.69, 138.41, 144.62, 145.37,151.12, 152.94, 156.49, 162.73 and 163.67) ppm.

2-((2-oxo-5-(3-(m-tolyl)ureido)indolin-3-ylidene)amino)nicotinamide (3b)

Physical properties: Reddish brown (75% yield); m.p. 270-273°C. FT-IR(KBr, cm^{-1}): 3312, 3223 cm^{-1} ν (NH of urea&2-oxoindolin), 3090,3020 cm^{-1} ν (C-H aromatic),2970,2856 cm^{-1} ν(C-H aliphatic), 1734 cm-1 ν (C=O), 1658 cm^{-1} ν (C=N+C=O of urea), 1610 cm^{-1} ν (C=C aromatic), 1562 cm^{-1} ν (NH deformation in urea), 1464 cm^{-1} ν (N-C-N) and 1310cm^{-1} ν(C-N).

^{1}H-NMR: 2.29ppm (s,3H, CH3), 6.81 ppm (m,2H, Ar-H), 6.93ppm (s,1H, Ar-H), 6.97ppm (d,1H, Ar-H), 7.00ppm (t,1H, Ar-H), 7.16ppm (s,2H, NH2)), 7.22ppm (m,3H, Ar-H) , 7.32ppm (d,1H, Ar-H) , 7.96ppm (d,1H, Ar-H) , 8.09ppm (s,1H, NH ureido) , 8.60 ppm (s,1H, NH ureido) and 10.96ppm (s,1H,NH).

^{13}C-NMR:(21.70, 115.78, 119.12, 122.98, 129.08, 138.41, 140.13, 151.02, 152.96, 156.50 and 163.67) ppm.

1-(2-oxo-3-((5-(trifluoromethyl)pyridin-2-yl)imino)indolin-5-yl)-3-(m-tolyl)urea (3c)

Physical properties: Orange (92% yield); m.p. 281–283°C. FT-IR(KBr, cm^{-1}): 3306, 3171 cm^{-1} ν (NH of urea&2-oxoindolin), 3073 cm^{-1} ν (C-H aromatic),2959,2851 cm^{-1} ν(C-H aliphatic), 1734 cm^{-1} ν (C=O), 1626 cm^{-1} ν (C=N+C=O of urea), 1612 cm^{-1} ν (C=C aromatic),1554 cm^{-1} ν (NH asymmetric deformation), 1468 cm^{-1} ν (N-C-N), 1296cm^{-1} ν(C-N) and 843cm^{-1} ν(C-F).

^{1}H-NMR: 2.29ppm (s,3H, CH3), 6.79 ppm (d,2H, Ar-H), 6.81ppm (t,1H, Ar-H), 6.98ppm (s,1H, Ar-H), 7.14ppm (d,1H, Ar-H), 7.17ppm (d,1H, Ar-H),7.19ppm (d,2H, Ar-H)), 7.24ppm (s,1H, Ar-H) , 7.27ppm (s,1H, Ar-H) , 7.34ppm (s,1H, NH ureido) , 8.90 ppm (s,1H, NH ureido) and 10.98ppm (s,1H,NH).

^{13}C-NMR:(21.70, 113.26, 113.38, 115.83,116.46, 119.18, 123.00, 123.36, 129.08, 131.87, 138.42,140.14, 144.66, 145.37, 151.12, 153.00, 156.51and 163.89) ppm.

1-(3-((4-(hydroxymethyl)pyridin-2-yl)imino)-2-oxoindolin-5-yl)-3-(m-tolyl)urea (3d)

Physical properties: Reddish orange (83.5% yield); m.p. 279-281°C. FT-IR(KBr, cm^{-1}): 3449cm^{-1} ν (OH), 3300,3184 cm^{-1} ν (NH of urea&2-oxoindolin), 3086cm-1 ν (C-H aromatic), 1734 cm^{-1} ν (C=O), 1635 cm^{-1} ν (C=N+C=O of urea), 1608 cm-1 ν (C=C aromatic), 1554 cm^{-1} ν (NH asymmetric deformation), 1487 cm^{-1} ν (N-C-N) and 1296cm^{-1} ν(C-N).

^{1}H-NMR: 2.30ppm (s,3H, CH3), 4.65 ppm (s,1H, OH), 6.54ppm (s,1H, Ar-H), 6.54ppm (s,1H, CH2 aliphatic), 6.79ppm (m,2H, Ar-H), 6.81ppm (s,1H, Ar-H), 7.14ppm (m,2H, Ar-H), 7.17ppm (d,1H, Ar-H)), 7.19ppm (d,2H, Ar-H) , 7.22ppm (s,1H, Ar-H) , 7.25ppm (d,1H, Ar-H), 7.33 ppm (s,1H, NH ureido), 8.58 ppm (s,1H, NH ureido) and 10.96ppm (s,1H,NH).

^{13}C-NMR:(21.71, 64.01, 115.81, 118.08, 119.16, 122.99, 129.08, 134.11, 138.41, 140.15, 143.21, 150.26, 152.97, 157.57, 161.19 and 163.58) ppm.

6-((5-(3-(2,6-dimethylphenyl)ureido)-2-oxoindolin-3-ylidene)amino)nicotinic acid (4a)

Physical properties: Reddish orange (81% yield); m.p. 298°C dec. FT-IR(KBr, cm^{-1}): 3267 cm^{-1} ν (NH of urea&2-oxoindolin), 3067 cm^{-1} ν (C-H aromatic),2918,2862 cm^{-1} ν(C-H aliphatic), 1734cm^{-1} ν (C=O), 1630 cm^{-1} ν (C=N+C=O of urea), 1553 cm^{-1} ν (NH asymmetric deformation), 1468 cm^{-1} ν (N-C-N) and 1304cm^{-1} ν(C-N).

^{1}H-NMR: 2.24ppm (s,6H, CH3), 6.44 ppm (m,3H, Ar-H), 6.94 ppm (d,3H, Ar-H), 6.96ppm (s,1H, Ar-H), 6.99ppm (d,1H, Ar-H), 7.05ppm (s,1H, Ar-H), 7.96ppm (s,1H, Ar-H), 8.93ppm (s,1H, NH ureido), 10.98ppm (s,1H, NH ureido) and 11.32ppm (s,1H,OH).

^{13}C-NMR:(18.67, 113.69, 115.81, 116.39, 119.15, 122.99, 123.97, 129.08, 131.68, 138.41, 140.15,144.72, 145.29, 150.18, 152.98, 163.68 and 166.76) ppm.

(Z)-2-((5-(3-(2,6-dimethylphenyl)ureido)-2-oxoindolin-3-ylidene)amino)nicotinamide(4b)

Physical properties: Red (82.4% yield); m.p. 222-224°C. FT-IR(KBr, cm^{-1}): 3371, 3273 cm^{-1} ν (NH of urea&2-oxoindolin),2980,2856 cm^{-1} ν(C-H aliphatic), 1732cm^{-1} ν (C=O), 1618 cm^{-1} ν (C=N+C=O of urea), 1554 cm^{-1} ν (NH asymmetric deformation), 1462cm^{-1} ν (N-C-N), 1311cm^{-1} ν(C-N).

^{1}H-NMR: 2.24ppm (s,6H, CH3), 6.57 ppm (m,3H, Ar-H), 6.93ppm (t,1H, Ar-H), 6.95ppm (s,2H, NH2), 6.96ppm (d,2H, Ar-H), 6.99ppm (s,1H, Ar-H), 7.05ppm (d,2H, Ar-H), 7.92 ppm (d,1H, Ar-H)), 7.95ppm (s,1H, NH ureido) , 8.07 ppm (s,1H, NH ureido), 10.98ppm (s,1H,NH).

^{13}C-NMR:(18.67, 113.30, 113.68, 116.38, 123.91, 128.11, 133.69, 137.51, 139.36, 144.68,145.27, 149.82, 152.61, 156.48 and 163.66) ppm.

1-(2,6-dimethylphenyl)-3-(2-oxo-3-((5-(trifluoromethyl)pyridin-2-yl)imino)indolin-5-yl)urea (4c)

Physical properties: Orange (88% yield); m.p. 287-289°C. FT-IR(KBr, cm^{-1}):3368, 3275 cm^{-1} ν (NH of urea&2-oxoindolin), 3064 cm^{-1} ν (C-H aromatic),2922,2853 cm^{-1} ν(C-H aliphatic), 1736 cm^{-1} ν (C=O), 1626 cm^{-1} ν (C=N+C=O of urea), 1618 cm^{-1} ν (C=C aromatic), 1553 cm^{-1} ν (NH asymmetric deformation), 1464 cm^{-1} ν (N-C-N), 1302cm^{-1} ν(C-N) and and845 cm^{-1} ν(C-F).

^{1}H-NMR: 2.26ppm (s,6H, CH3), 6.67 ppm (d,1H, Ar-H), 6.73 ppm (m,3H, Ar-H), 6.94ppm (d,1H, Ar-H), 6.97ppm (d,2H, Ar-H), 7.00ppm (s,1H, Ar-H),

7.06ppm (s,1H, Ar-H), 7.97ppm (s,1H, NH ureido), 8.67ppm (s,1H, NH ureido)and 10.97 ppm (s,1H, NH).

^{13}C-NMR:(18.67, 113.29, 113.73, 116.42, 123.86, 128.13, 134.36, 137.97, 144.67,145.33, 150.04, 152.45, 156.49 and 163.67) ppm.

1-(2,6-dimethylphenyl)-3-(3-((4-**(hydroxymethyl)pyridin-2-yl)imino)-2-oxoindolin-5-yl)urea (4d)**

Physical properties: Orange (80% yield); m.p. 273-275°C. FT-IR(KBr, cm^{-1}): 3441cm^{-1} ν (OH),3375, 3279 cm^{-1} ν (NH of urea&2-oxoindolin), 2964,2856 cm^{-1} ν(C-H aliphatic), 1734 cm^{-1} ν (C=O), 1626 cm^{-1} ν (C=N+C=O of urea),), 1553 cm^{-1} ν (NH asymmetric deformation), 1462 cm^{-1} ν (N-C-N), 1298cm^{-1} ν(C-N).

^{1}H-NMR: 2.26ppm (s,6H, CH3), 4.41 ppm (s,1H, OH), 6.45 ppm (s,2H, CH2 aliphatic), 6.52ppm (m,3H, Ar-H), 6.73ppm (s,1H, Ar-H), 6.94ppm (d,1H, Ar-H), 6.98ppm (d,2H, Ar-H), 7.01ppm (s,1H, Ar-H), 7.06ppm (d,1H, Ar-H)), 7.83ppm (s,1H, NH ureido) , 8.56 ppm (s,1H, NH ureido), 10.98ppm (s,1H,NH).

^{13}C-NMR:(18.67, 64.78, 113.32, 113.69, 116.93, 123.93, 128.12, 135.91, 144.70,145.29, 150.40, 152.69, 156.49, 160.95 and 163.67) ppm.

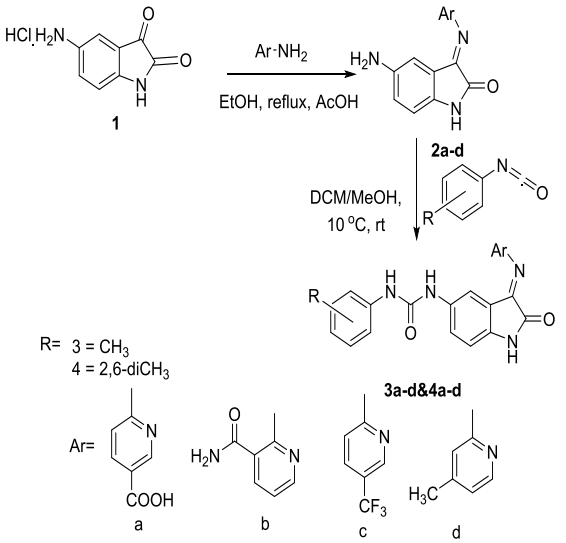

Scheme 1: Synthesis of Schiff bases and target compounds

2.2. In vitro anticancer activity:

The MTT colorimetric assay was used to estimate the effects of synthesized compounds **(3a-d&4a-d)** on lung cancer cell viability. Cells suspension (100µL) were added into 96-well flat-bottom tissue culture plated at concentrations of (5 x 10^3 cells per well) and incubated for (24hr.) in standard conditions, (4 x 10^3 cells per well) for 48hr, and (3 x 10^3 cells per well) for 72hr incubation. Afterward, 24hr completed the cells were treated with 50 µM from each compound from each compound.

When a recovery period of 24hr, 48hr, and 72hr, completed the cell culture medium was removed and cultures were incubated for 4hr at 37 Cº with a medium containing 20µL of MTT (of stock of 5mg/mL MTT/PBS from 30mL solution). After 4hr remove the supernatant and dispose it according to the lab recommendations. Add 100µL of DMSO to each well to solubilize the crystals and tap the plates onto roll paper; leave the plates open and facing down to the paper at room temperature in the dark condition for about (15-20 min) , and repeat this section in 48 and 72hr.

The assay was done in a triplicate and the optical density of each plate (well) was measured at a transmitting wavelength (520-600 nm) by using Multiscan Reader. The inhibition rate of cell growth (percentage of cytotoxicity) was calculated as follows:

[Inhibition Rate percentage= (A-B/A)*100]

Where [A, and B] referred to the optical density of control & tested compounds respectively[20].

2.3. Computational methods:

CCDC GOLD Suite (*v*.5.7.1) was utilized to perform the molecular docking researchs for the compounds. CCDC Hermes visualizer software (*v*. 1.10.1) was utilized to imagine: the protein, ligands, hydrogen bonding interactions, short contacts and bonds length calculation. The chemical structures of our ligands were drawn utilizing ChemBioOffice (*v*. 17.1) software. The pharmacokinetic profile, i.e., ADME of the synthesized compounds was anticipated with the assistance of swiss ADME server [21] .

2.4. ADME procedures

All final ligands **(3a-d&4a-d)** were drawn by Chem Sketch (*v*. 12), converted to SMILE name by Swiss ADME tool which predicts the physicochemical descriptors and pharmacokinetic properties. BOILEDEGG was used to compute the lipophilicity and polarity of the small molecule[22].

2.5. Docking procedures:

Setup of the receptors for the docking process done by using Hermes visualizer software in the CCDC GOLD suite. Determination of the active site is according to the original ligand interaction site. The protein binding site with all the protein residues

defined within the (10 A°) of the reference ligand for the docking process.

All parameters used during the docking procedure chosen as default settings. The number of generated poses was fixed as 10, while the top ranked solution was kept as default, also the early termination option was turned off. Chemscore kinase was used as a configuration template. While the piecewise linear potential (CHEMPLP) is used as a scoring function.

GOLD outputs docking results in terms of a fitness score. The higher the fitness is, the better the docked interaction between a protein and a ligand. Finally, the results were saved as mol.2 files; that provide informations about the best binding manner, the free energy of binding and docked poses. These results were studied precisely to define the best binding and interaction of our designed ligand with amino acid residues of receptor (EGFR) [23&24].

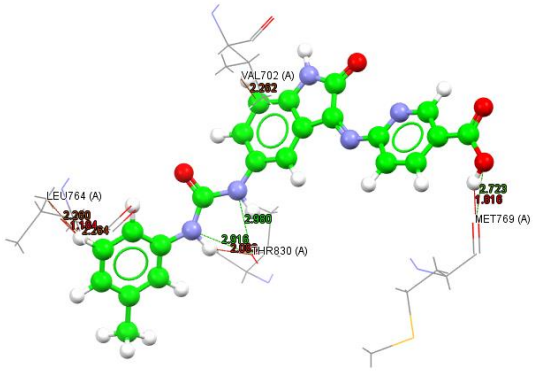

Figure (1) H-bond and short contact interaction profile for the compound 3a binding with EGFR receptor (PDB code: 4HJO). The interaction between 3a and amino acid residues by H-bond [The 830,Met 769] represents in a green while for short contact in red [Met 769, Thr 830,Leu 764, Val 703] . [3a: ball and stick style, amino acid residues in wireframe style]

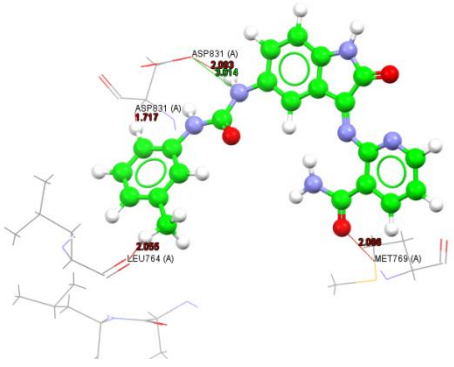

Figure (2) H-bond and short contact interaction profile for the compound 3b binding with EGFR receptor (PDB code: 4HJO). The interaction between 3b and amino acid residues by H-bond [Asp 831] represents in a green while for short contact in red [Asp 831, Met 769, Leu 764] . [3b : ball and stick style, amino acid residues in wireframe style]

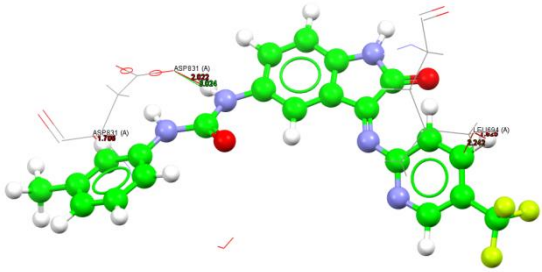

Figure (3) H-bond and short contact interaction profile for the compound 3c binding with EGFR receptor (PDB code: 4HJO). The interaction between 3c and amino acid residues by H-bond [Thr 830] represents in a green while for short contact in red [Val 702, Thr 830, Leu 764, Leu 694] . [3c : ball and stick style, amino acid residues in wireframe style]

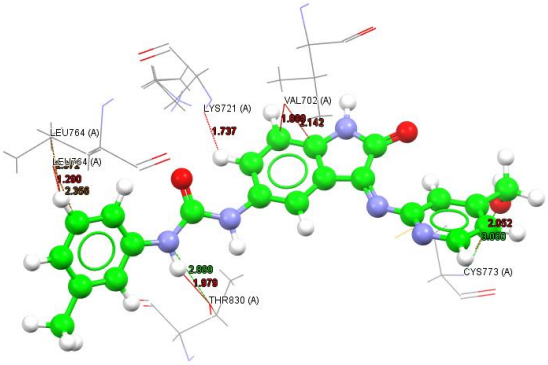

Figure (4) H-bond and short contact interaction profile for the compound 3d binding with EGFR receptor (PDB code: 4HJO). The interaction between 3d and amino acid residues by H-bond [Thr 830, Cys 773] represents in a green while for short contact in red [Cys 773, Val 702, Lys 721, Thr 830, Leu 764] . [3d: ball and stick style, amino acid residues in wireframe style]

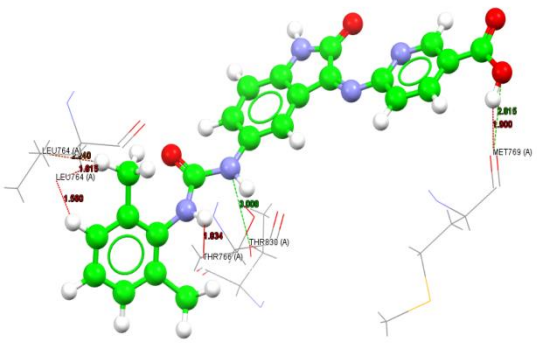

Figure (5) H-bond and short contact interaction profile for the compound 4a binding with EGFR receptor (PDB code: 4HJO). The interaction between 4a and amino acid residues by H-bond [The 830, Met 769] represents in a green while for short contact in red [Thr 766, Met 769, Leu 764]. [4a: ball and stick style, amino acid residues in wireframe style]

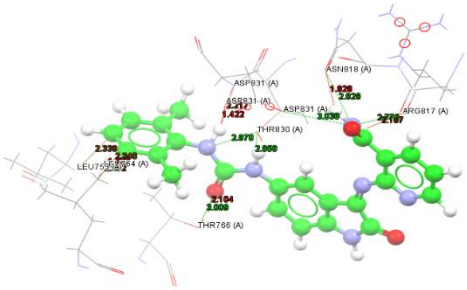

Figure (6) H-bond and short contact interaction profile for the compound 4b binding with EGFR receptor (PDB code: 4HJO). The interaction between 4b and amino acid residues by H-bond [Asn 818, Asp 831, Arg 817, Thr 766, Thr 830] represents in a green while for short contact in red [Arg 817, Asn 818, Thr 766, Asp831, Leu 753, Leu]. [4b: ball and stick style, amino acid residues in wireframe style]

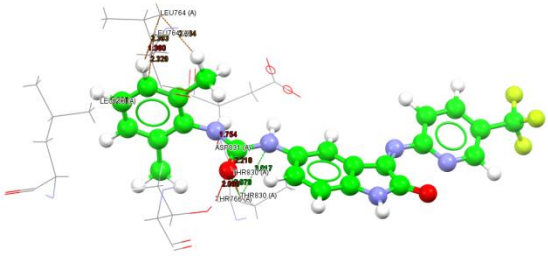

Figure (7) H-bond and short contact interaction profile for the compound 4c binding with EGFR receptor (PDB code: 4HJO). The interaction between 4c and amino acid residues by H-bond [Thr 830] represents in a green while for short contact in red [Leu 753, Leu 764, Thr 830, Thr 766, Asp 831]. [4c: ball and stick style, amino acid residues in wireframe style]

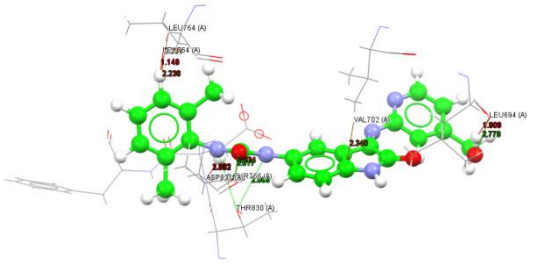

Figure (8) H-bond and short contact interaction profile for the compound 4d binding with EGFR receptor (PDB code: 4HJO). The interaction between 4d and amino acid residues by H-bond [Thr 830, Thr 766, Leu 694] represents in a green while for short contact in red [Thr 766, Leu 764, Asp 831, Leu 694, Val 702]. [4d: ball and stick style, amino acid residues in wireframe style]

ADME Studies:

The pharmacokinetic properties of all produced substances were evaluated (absorption, distribution, metabolism, excretion and toxicity).

Topological polar surface area (TPSA) was estimated, which is a very useful descriptor to estimate some ADME properties specially the degree of drug bioavailability and brain access[25].Thus, the molecules with a TPSA >140 A^{o} are thought to have low gastrointestinal absorption. The results of all our synthesized compounds showed that TPSA values less than 140, which is in the range (**138.57–95.48**) and the bioavailability for all ligands is in the range **(0.56 –0.55)** which mean that all ligands reach the systemic circulation, as shown in the **Table 2**. All the final compounds **(3a-d&4a-d)** fulfilled Lipinski rule, it also fulfilled the topological descriptors and fingerprints of molecular drug-likeness structure keys as Log P and Log S.

Table (1) The binding energies for ureidoindolin-2-one derivatives (3a-d&4a-d)and standard TKIs Erlotinib docked with EGFR

Compounds	*EGFR Binding Energy (PLP Fitness)*	*Amino Acids Included in H- bonding*	*Amino Acids Included in short contact Interactions*
3a	85.1	The 830 (2)*, Met 769	Met 769, Thr 830, Leu 764 (3)*, Val 703

3b	80.36	Asp 831	Asp 831(2)*, Met 769, Leu 764
3c	82.35	Asp 831	Asp 831(2)* , Leu 694(2)*
3d	80.28	Thr 830, Cys 773	Cys 773, Val 702(2)*, Lys 721, Thr 830, Leu 764(3)*
4a	81.80	The 830, et 769	Thr 766, Met 769, Leu 764 (3)*
4b	77.43	Asn 818, Asp 831, Arg 817, Thr 766, Thr 830 (2)*	Arg 817, Asn 818, Thr 766, Asp831(2)*, Leu 753, Leu 764 (3)*
4c	78.49	Thr 830 (2)*	Leu 753, Leu 764(4)*, Thr 830, Thr 766, Asp 831
4d	76.45	Thr 830 (2)*, Thr 766, Leu 694	Thr 766, Leu 764(3)*, Asp 831 (2)*, Leu 694, Val 702
Erlotinib	83.94	Met 769, Lys 704	Gly695(2)*, Lys 692, Leu 694 (2)*, Met 769, Leu 764

*Number in brackets refers to the number of bonds with the same aminoacid

Table 2: ADME properties profile of the synthesized compounds (3a-d&4a-d)

Compounds	Formula	M.Wt (g/mol)	H-bond acceptors	H-bond donors	MR	TPSA	GI Abs.	BBB permeant	Lipiniski violations
3a	$C_{22}H_{17}N_5O_4$	**415.41**	**6**	**4**	**118.91**	**132.78Å²**	**high**	**No**	**0**
3b	$C_{22}H_{18}N_6O_3$	**414.43**	**5**	**4**	**120.04**	**138.57Å²**	**high**	**No**	**0**
3c	$C_{22}H_{16}F_3N_5O_2$	**439.40**	**7**	**3**	**116.95**	**95.48Å²**	**high**	**No**	**0**
3d	$C_{22}H_{19}N_5O_3$	**401.42**	**5**	**4**	**118.07**	**115.71Å²**	**high**	**No**	**0**
4a	$C_{23}H_{19}N_5O_4$	**429.44**	**6**	**4**	**123.87**	**132.78Å²**	**high**	**No**	**0**
4b	$C_{23}H_{20}N_6O_3$	**428.45**	**5**	**4**	**125.01**	**138.57Å²**	**high**	**No**	**0**
4c	$C_{23}H_{18}F_3N_5O_2$	**453.43**	**7**	**3**	**121.92**	**95.48 Å²**	**high**	**No**	**0**
4d	$C_{23}H_{21}N_5O_3$	**415.45**	**5**	**4**	**123.04**	**115.71Å²**	**high**	**No**	**0**

3. Results and Discussion:

5- aminoisatin Schiff bases **(2a-d)** were synthesized by cyclocondensation reaction using conventional method; compounds **(3a-d&4a-d)**were synthesized by reacting 5-aminoisatin Schiff bases **(2a-d)** with the appropriate aromatic isocyanates.

The synthesized compounds were characterized by FT- IR and ^{1}H NMR, ^{13}C NMR techniques. The IR spectrum of Schiff bases **(2a-d)** showed disappearance of absorption band due to ν (C=O) ketone of 2-oxoindolin at 1763 cm^{-1} and appearance of ν (C=N) absorption band at (1661-1657) cm^{-1} is an evidence of Schiff bases formation . The spectrum shows other bands at (3445-3271) cm^{-1}; (3225-3184) cm^{-1}; (1734-1732) cm^{-1}; due to ν (NH_2) of isatin, ν (NH) of oxoindole and ν (C=O) of oxoindole respectively.

^{1}H-NMR spectra of compounds **(2a-d)** showed singlet signal at δ = (10.95-10.63) ppm due to (NH) proton of 2-oxoindolin; and signals at δ = (10.62-6.48) ppm due to aromatic protons and singlet signal at δ = (5.80) ppm due to NH_2 of isatin. ^{1}H-NMR spectrum data of compound 2a& 2d showed singlet signal at δ = (10.96&4.43) ppm respectively due to proton of hydroxyl group; ^{13}C-NMR spectral data of compounds **(2a-d)** showed disappearance of signal at δ = (185.89) ppm due to ketonic (C=O) of 2-oxoindolin and appearance of signal at δ = (156.49-156.48.6) ppm due to (C=N).

While the FTIR spectra of compounds **(3a-d&4a-d)**showed disappearance of absorption band due to ν (NH_2) of isatin (3485-3275) cm^{-1} and the appearance of absorption band due to ν (NH) symmetric stretching and ν (C=O) of urea at (3375-3171) cm^{-1}; (1658-1618) respectively.

^{1}H-NMR spectra of compounds **(3a-d&4a-d)** showed two singlet signal at δ = (8.99-8.07)&(8.09-7.33) ppm due to (NH) proton of ureido group; singlet signal at δ = (2.30-2.24) ppm due to protons of CH_3 substitution also the spectrum showed disappearance of signal at δ = (5.80) ppm due to NH_2 of isatin, ^{13}C-NMR spectra of compounds **(3a-d&4a-d)**showed appearance of signal at δ = (153.00-152.45) ppm due to (C=O) of ureido group and signal at δ = (21.86-18.67) ppm due to carbon of CH_3 substitution.

The obtained data revealed that from the the newly synthesized compounds **[3a& 3d]** had an inhibitory activity against A549 cancer cell with a relative inhibition percentage (30.4&40.9 μM) respectively that was close to the approved drug, erlotinib (25.23 μM) while the other synthesized compound had not shown a promising inhibitory activity against A549 cancer cell and compound 4a is an example for them; there is a good agreement between our docked results and the experimental results (*In vitro* study) since the two compounds that show the highest docking results are the same that

show a promising antitumor activities among the tested compounds.

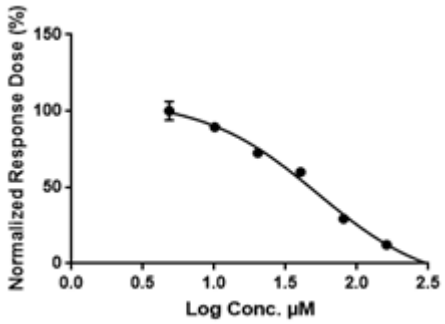

Compound 3a, IC_{50} (µM)= 30.4

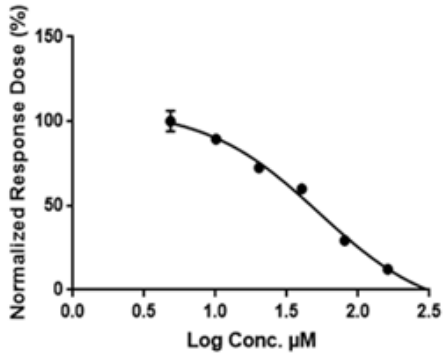

Compound 3d, IC_{50} (µM)= 40.9

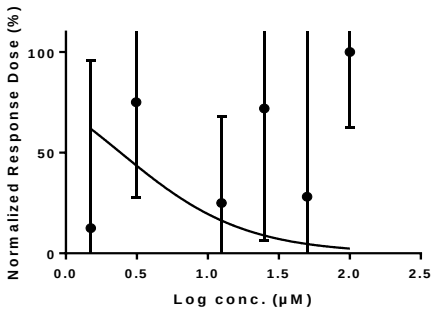

Compound 4a, IC50 (µM) >100µM

Figure (9) Dose-response curves of IC_{50} for A549 for compounds **[3a, 3d&4a]**, treated for 72hr. with different ranges of concentrations (100, 50, 25, 12.5, 6.25, 3.125, 1.562, 0.781, 0.390, and, 0.195 µM). The normalized dose-response was plotted with log concentrations of compounds **[3a,3d& 4a]**. The determination of IC_{50} values was done using nonlinear regression analysis (prism). Error bars represent the standard error of the mean% (SEM) for triplicate analysis

Conclusion:

1. The synthesis of the designed compounds has been successfully achieved.
2. The effects of synthesized compounds **(3a-d&4a-d)**, on human A549 (lung) cancer cell line that is examined by MTT colorimetric assay showed that compounds **[3a& 3d]** have inhibitory activity against A549 cancer cell with inhibition percentage comparable to the standard drug erlotinib and these results correspond to the results in the Gold program. While other synthesized compounds shows no acceptable inhibitory activity against A549 cancer cell. Also ADME studies showed all final compounds **(3a-d&4a-d)** fulfilled the Lipinski rule, and all synthesized compounds absorbed from GIT.

Acknowledgement:

The authors would like to thank Mustansiriyah University (www.uomustansiriyah.edu.iq) Baghdad-Iraq for its support in the present work.

REFERENCES:

[1] Rajarshi N, Shelly P, Gourav G, Md Jawaid A. Isatin containing heterocycles for different biological activities: Analysis of structure activity relationship. Journal of Molecular Structure. 2020; (1222):128900.

[2] Vinod U, Harun P, Bijal P, Sanjay B. Benzofurano-isatins: Search for antimicrobial agents. Arabian Journal of Chemistry. 2017; 10: S389–S396.

[3] Marzieh RK, Ahmad MF, Aref M, Alireza A. Synthesis and evaluation of anticonvulsant activity of (Z)-4-(2-oxoindolin-3-ylideneamino)-N-phenylbenzamide derivatives in mice. Research in Pharmaceutical Sciences. 2018 June; 13(3): 262-272.

[4] Huda SS , Hatem AA, Iman SI, Amany ZM, Ali H, Md A, Motiur RAFM. Synthesis of novel potent biologically active N-benzylisatin-aryl hydrazones in comparison with lung cancer drug 'gefitinib'. Appl. Sci. 2020 May; 10(3669).

[5] Ravi J, Kiran G, Sarangapani M, Sriram R. Synthesis, in vivo anti-inflammatory activity, and molecular docking studies of new isatin derivatives. International Journal of Medicinal Chemistry. 2016.

[6] Ozougwu, Jevas C. The Role of Reactive Oxygen Species and Antioxidants in Oxidative Stress. International Journal of Research in Pharmacy and Biosciences. 2016 June; 6(3): 1-8.

[7] Aleti R, Srinivas MM. Synthesis, characterization, and anthelmintic activity of novel benzothiazole derivatives containing indole moieties. Asian J Pharm Clin Res. 2019; 3(12): 321-325.

[8] Milica MB, Marko C˘B. Classification of brain tumors from MRI images using a convolutional neural network. Appl. Sci. 2020;10:1999.

[9] Tarini S. Tumors: Benign and Malignant. Canc Therapy & Oncol Int J. 2018 May; 10(3).

[10] Satoshi Y, Takayoshi K, Takamasa T, Taichi S, Hadrien C, Yasuo K, Takeshi N, Yi-Chia L, Naoko I, Masahiro M, Naoko H, Hideyuki T, Reiko N, Ichiro O, Shoichiro T, Ming-Shiang W, Toshikazu U. Genetic and epigenetic alterations in normal tissues have differential impacts on cancer risk among tissues.PNAS. 2018 Feb 6; 115(6): 1328–1333.

[11] Hideyuki T, Toshikazu U. Accumulation of genetic and epigenetic alterations in normal cells and cancer risk. npj Precision Oncology. 2019; 3 (7).

[12] Sevinci P, Ana ME, Isabela T, Elvira G, Cristiana T. Phytochemicals in cancer prevention: modulating epigenetic alterations of DNA methylation. Phytochem Rev. 2019 July10; 18:1005–1024.

[13] Agnes AF. Mapmaking and mapthinking: cancer as a problem of place in nineteenth-century England. Social History of Medicine. 2018; 33(2): 463–488.

[14] David EG, Armen HT, Ehrin JA, April WA. Principles of pharmacology the pathophysiologic basis of drug therapy. 3rd Edition. Lippincott williams & wilkins: Philadelphia; 2012: 563.

[15] Laurence LB, Bruce AC, Bjorn CK. Goodman& Gilman's the pharmacological basis of therapeutics.12th Edition. McGraw-Hill Education; 2011:1671.

[16] Deepak K, Mrunal S. Synthesis and evaluation of antimicrobial, antitubercular and anticancer activities of dihydrobenzimidazole thiopyranooxazinone derivatives. Research J. Pharm. and Tech. 2021; 14(3):1453-1458.

[17] Daina A, Michielin O, Zoete V. SwissADME: a free web tool to evaluate pharmacokinetics, drug-likeness and medicinal chemistry friendliness of small molecules. Scientific reports. 2017Mar 3; 7: 42717.

[18] Kamaleddin HE Tehrani, Maryam H, M H, Farzad K , Shohreh M. Synthesis and antibacterial activity of Schiff bases of 5-substituted isatins. Chinese Chemical Letters. 2016; 27: 221–225.

[19] Rahul RK , Grace SC, Hsiao-CW, Chao-WY, Chiung-HH, On Lee , Chih-HC, Chrong-SH, Ching-HK, Nien-TC, Mai-WL,Ling-MW, Yen-CC , Tzong-HH, Chia-NC, Hui-CH, Hui CL,Ying-CS, Shuen-HC, Hsiang-WT, Chih-PL, Chia-MT, Tsan-LH, Yuan-JT, Ji-WC. Synthesis and structure–activity relationship of 6-arylureido-3-pyrrol-2-ylmethylideneindolin-2-one derivatives as potent receptor tyrosine kinase inhibitors. Bioorganic & Medicinal Chemistry .2010; 18: 4674–4686.

[20] Shakila BS, Krishnamoorthy G, Senthamarai R, Mohamed JMS. Synthesis, spectral characterization and anticancer activity of novel pyrimidine derivatives. Research J. Pharm. and Tech. 2020; 13(12):6243-6247.

[21] Duha ET, Ayad MRR, Karima FA. Design,synthesis, characterization, biological activity and ADME study of new 5-arylidene-4-thiazolidinones derivatives having Nabumetone moiety. Al Mustansiriyah Journal of Pharmaceutical Sciences. 2019;19(4):77.

[22] Daina A, Zoete V. A BOILED- Egg to predict gastrointestinal absorption and brain penetration of small molecules.ChemMedChem. 2016 Jun 6; 11(11):1117-21.

[23] Mustafa MA, Monther FM, Ayad MRR. Synthesis, anti-inflammatory, molecular docking and ADME studies of new derivatives of ketoprofen as cyclooxygenases inhibitor. Al Mustansiriyah Journal of Pharmaceutical Sciences. 2019; 19(4).

[24] Sarah SI, Monther FM, Basma MA. Molecular drug design, synthesis and antibacterial study of novel 4-oxothiazolidin-3-yl derivatives. Al-Mustansiriyah Journal of Pharmaceutical Sciences. 2020 June ; 20(2):1- 10.

[25] Abdul Muhaimen AA, Monther FM, Ayad KK. Design, synthesis and acute anti-inflammatory assessment of new2-methyl benzoimidazole derivatives having 4-thiazolidinone nucleus. Al Mustansiriyah Journal of Pharmaceutical Sciences. 2019; 19(4): 151.